Dynamics of the vitreous humour induced by eye rotations: implications for retinal detachment and intra-vitreal drug delivery

Jan Pralits

Department of Civil, Chemical and Environmental Engineering
University of Genoa, Italy
jan.pralits@unige.it

October 19, 2013

The work presented has been carried out by:

- **Rodolfo Repetto** DICCA, University of Genoa, Italy;
- **Jennifer Siggers** Imperial College London, UK;
- **Jan Pralits** DICCA, University of Genoa, Italy;
- **Alessandro Stocchino** DICCA, University of Genoa, Italy;
- **Krystyna Isakova** DICCA, University of Genoa, Italy;
- **Julia Meskauskas** DISAT, University of L'Aquila, Italy;
- **Andrea Bonfiglio** DICCA, University of Genoa, Italy.

Anatomy of the eye

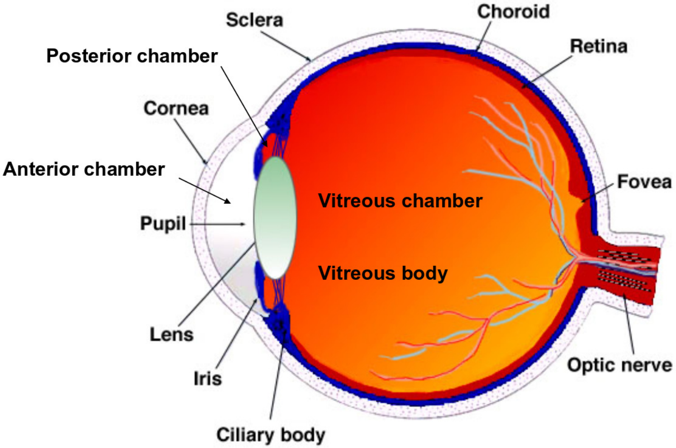

Vitreous characteristics and functions

Vitreous composition

The main constituents are

- Water (99%);
- hyaluronic acid (HA);
- collagen fibrils.

Its structure consists of long, thick, non-branching collagen fibrils suspended in hyaluronic acid.

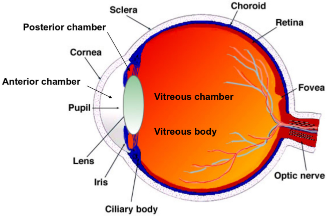

Normal vitreous characteristics

- The healthy vitreous in youth is a gel-like material with **visco-elastic mechanical properties**, which have been measured by several authors (Lee et al., 1992; Nickerson et al., 2008; Swindle et al., 2008).
- In the outermost part of the vitreous, named **vitreous cortex**, the concentration of collagen fibrils and HA is higher.
- The vitreous cortex is in contact with the **Internal Limiting Membrane (ILM)** of the retina.

Physiological roles of the vitreous

- **Support function for the retina** and filling-up function for the vitreous body cavity;
- **diffusion barrier** between the anterior and posterior segment of the eye;
- establishment of an **unhindered path of light.**

Vitreous ageing

With advancing age the vitreous typically undergoes significant changes in structure.

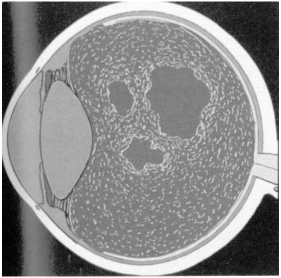

- Disintegration of the gel structure which leads to **vitreous liquefaction (synchisys)**. This leads to an approximately linear increase in the volume of liquid vitreous with time. Liquefaction can be as much extended as to interest the whole vitreous chamber.

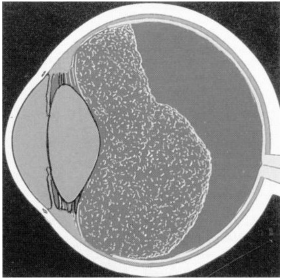

- Shrinking of the vitreous gel **(syneresis)** leading to the detachment of the gel vitreous from the retina in certain regions of the vitreous chamber. This process typically occurs in the posterior segment of the eye and is called **posterior vitreous detachment (PVD)**. It is a pathophysiologic condition of the vitreous.

Partial vitreous liquefaction

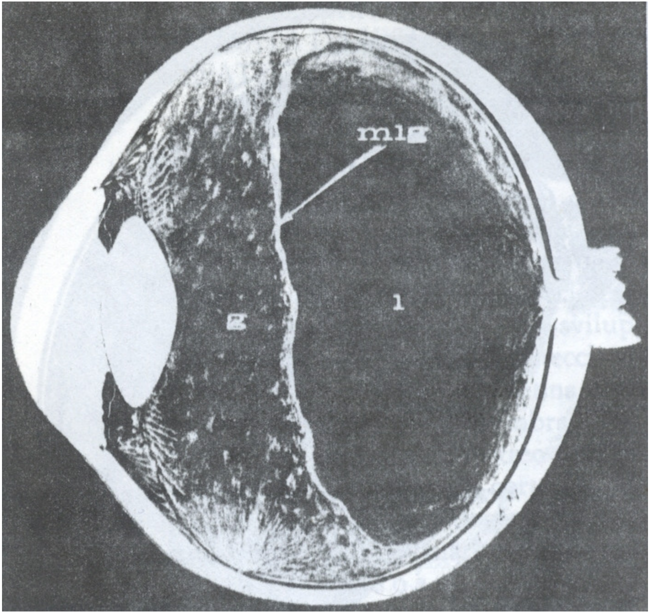

Retinal detachment

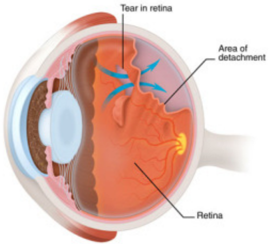

Posterior vitreous detachment (PVD) and vitreous degeneration:

- more common in myopic eyes;
- preceded by changes in vitreous macromolecular structure and in vitreoretinal interface → possibly mechanical reasons.
- If the retina detaches from the underlying layers → loss of vision;

Rhegmatogeneous retinal detachment:

- fluid enters through a retinal break into the sub retinal space and peels off the retina.

Risk factors:

- **myopia;**
- posterior vitreous detachment (PVD);
- lattice degeneration;
- ...

Scleral buckling and vitrectomy

Scleral bluckling

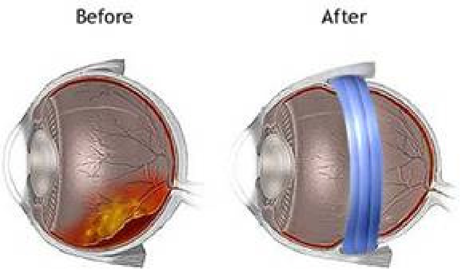

Scleral buckling is the application of a rubber band around the eyeball at the site of a retinal tear in order to promote reachtachment of the retina.

Vitrectomy

The vitreous may be completely replaced with tamponade fluids: silicon oils, water, gas, ..., usually immiscible with the eye's own aqueous humor

Intravitreal drug delivery

It is difficult to transport drugs to the retina from 'the outside' due to the tight blood-retinal barrier → use of **intravitreal drug injections.**

Diffusion is usually understood as the principal source for drug delivery, what about **advection** ?

Motivations of the work

Why do research on vitreous motion?

- Possible connections between the mechanism of **retinal detachment** and
    - the shear stress on the retina;
    - flow characteristics.
- Especially in the case of liquefied vitreous eye rotations may produce effective **fluid mixing**. In this case **advection may be more important that diffusion** for mass transport within the vitreous chamber.
  Understanding diffusion/dispersion processes in the vitreous chamber is important to predict the behaviour of drugs directly injected into the vitreous.

The effect of viscosity

Main working assumptions

- **Newtonian fluid**
  The assumption of purely viscous fluid applies to the cases of
  - vitreous liquefaction;
  - substitution of the vitreous with viscous tamponade fluids .
- **Sinusoidal eye rotations**
  Using dimensional analysis it can be shown that the problem is governed by the following two dimensionless parameters

$$\alpha = \sqrt{\frac{R_0^2 \omega_0}{\nu}} \qquad \textbf{Womersley number},$$

$$\varepsilon \qquad \textbf{Amplitude of oscillations}.$$

- **Spherical domain**

Theoretical model I

David et al. (1998)

Scalings

$$\mathbf{u} = \frac{\mathbf{u}^*}{\omega_0 R_0}, \quad t = t^* \omega_0, \quad r = \frac{r^*}{R_0}, \quad p = \frac{p^*}{\mu \omega_0},$$

where ω_0 denotes the angular frequency of the domain oscillations, R_0 the sphere radius and μ the dynamic viscosity of the fluid.

Dimensionless equations

$$\alpha^2 \frac{\partial}{\partial t}\mathbf{u} + \alpha^2 \mathbf{u} \cdot \boldsymbol{\nabla}\mathbf{u} + \boldsymbol{\nabla} p - \nabla^2 \mathbf{u} = 0, \qquad \boldsymbol{\nabla} \cdot \mathbf{u} = 0, \tag{1}$$

$$u = v = 0, \quad w = \varepsilon \sin\vartheta \sin t \qquad (r = 1), \tag{2}$$

where ε is the amplitude of oscillations. **We assume $\varepsilon \ll 1$.**

Asymptotic expansion

$$\mathbf{u} = \varepsilon \mathbf{u}_1 + \varepsilon^2 \mathbf{u}_2 + \mathcal{O}(\varepsilon^3), \quad p = \varepsilon p_1 + \varepsilon^2 p_2 + \mathcal{O}(\varepsilon^3).$$

Since the equations and boundary conditions for u_1, v_1 and p_1 are homogeneous the solution is $p_1 = u_1 = v_1 = 0$.

Theoretical model II

Velocity profiles on the plane orthogonal to the axis of rotation at different times.

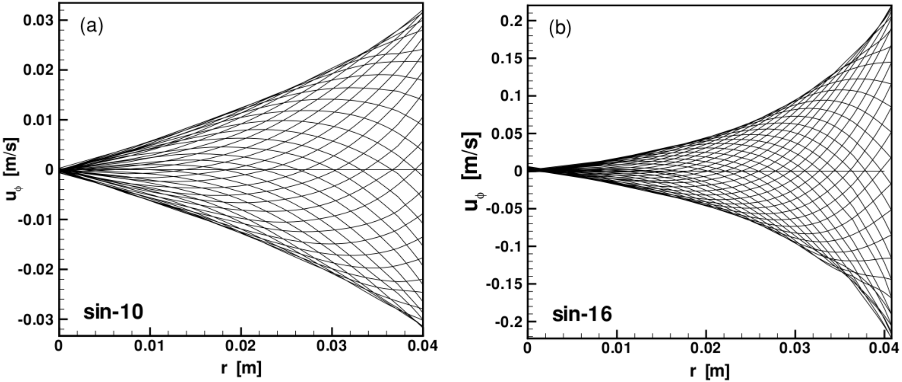

- Limit of small α: **rigid body rotation;**
- Limit of large α: formation of an **oscillatory boundary layer at the wall.**

Experimental apparatus I

Repetto et al. (2005), Phys. Med. Biol.
The experimental apparatus is located at the University of Genoa.

- Perspex cylindrical container.
- Spherical cavity with radius $R_0 = 40$ mm.
- Glycerol (highly viscous Newtonian fluid).

Experimental apparatus II

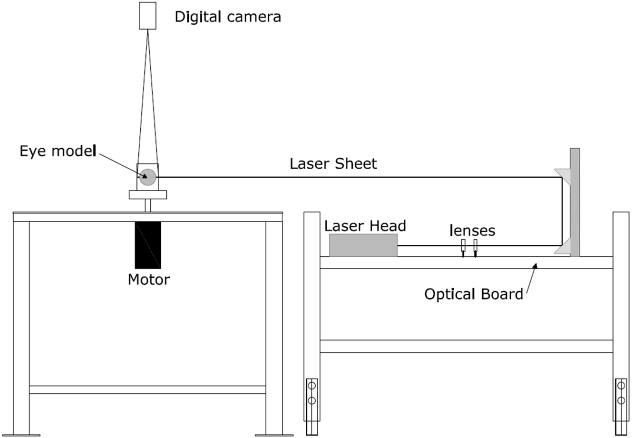

Experimental measurements

Typical PIV flow field

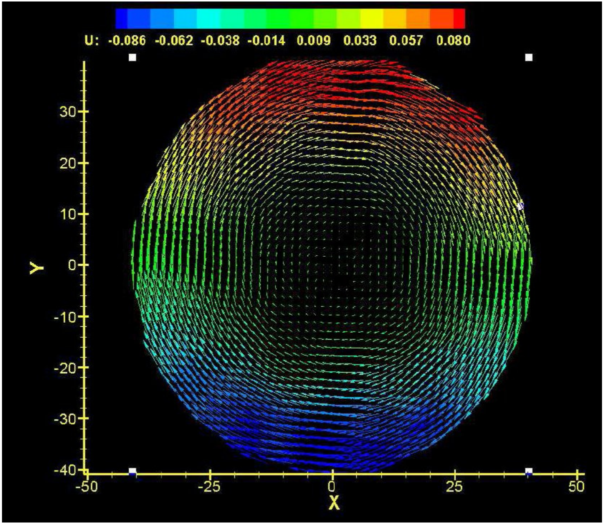

Comparison between experimental and theoretical results

Radial profiles of $\Re(g_1)$, $\Im(g_1)$ and $|g_1|$ for two values of the Womersley number α.

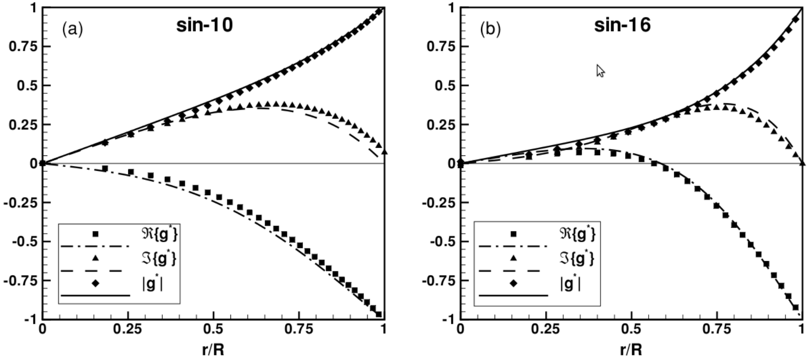

The case of a viscoelastic fluid I

- As we deal with an sinusoidally oscillating linear flow we can obtain the solution for the motion of a viscoelastic fluid simply by replacing the real viscosity with a **complex viscosity.**
- In terms of our dimensionless solution this implies introducing a **complex Womersley number.**
- Rheological properties of the vitreous (complex viscosity) can be obtained from the works of Lee et al. (1992), Nickerson et al. (2008) and Swindle et al. (2008).
- It can be proved that in this case, due to the presence of an elastic component of vitreous behaviour, the system admits natural frequencies that can be excited resonantly by eye rotations.

Formulation of the problem I

The motion of the fluid is governed by the momentum equation and the continuity equation:

$$\frac{\partial \mathbf{u}}{\partial t} + (\mathbf{u} \cdot \nabla)\mathbf{u} + \frac{1}{\rho}\nabla p - \frac{1}{\rho}\nabla \cdot \mathbf{d} = 0, \tag{3a}$$

$$\nabla \cdot \mathbf{u} = 0, \tag{3b}$$

where $\mathbf{d}$ is the deviatoric part of the stress tensor.

Assumptions

- We assume that the velocity is small so that nonlinear terms in (3a) are negligible.
- For a linear viscoelastic fluid we can write

$$\mathbf{d}(t) = 2\int_{-\infty}^{t} G(t-\tilde{t})\mathbf{D}(\tilde{t})d\tilde{t} \tag{4}$$

  where $\mathbf{D}$ is the rate of deformation tensor and G is the relaxation modulus.

Therefore we need to solve the following problem

$$\rho\frac{\partial \mathbf{u}}{\partial t} + \nabla p - \int_{-\infty}^{t} G(t-\tilde{t})\nabla^2\mathbf{u}\; d\tilde{t} = 0, \tag{5a}$$

$$\nabla \cdot \mathbf{u} = 0, \tag{5b}$$

Relaxation behaviour I

We assume that the solution has the structure

$$\mathbf{u}(\mathbf{x}, t) = \mathbf{u}_\lambda(\mathbf{x}) e^{\lambda t} + c.c., \qquad p(\mathbf{x}, t) = p_\lambda(\mathbf{x}) e^{\lambda t} + c.c.,$$

where $\mathbf{u}_\lambda, p_\lambda$ do not depend on time and $\lambda \in \mathbb{C}$.
It can be shown that the deviatoric part of the stress tensor takes the form

$$\mathbf{d}(t) = 2 \int_{-\infty}^{t} G(t - \tilde{t}) \mathbf{D}(\tilde{t}) d\tilde{t} = 2\mathbf{D} \frac{\tilde{G}(\lambda)}{\lambda}, \tag{6}$$

where

$$\tilde{G}(\lambda) = G'(\lambda) + iG''(\lambda) = \lambda \int_0^\infty G(s) e^{-\lambda s} ds$$

is the complex modulus.

- G': **storage modulus;**
- G'': **loss modulus;**

This leads to the eigenvalue problem

$$\rho \lambda \mathbf{u}_\lambda = -\nabla p_\lambda + \frac{\tilde{G}(\lambda)}{\lambda} \nabla^2 \mathbf{u}_\lambda, \quad \nabla \cdot \mathbf{u}_\lambda = 0, \tag{7}$$

which has to be solved imposing **stationary no-slip conditions** at the wall and **regularity conditions** at the origin.

Relaxation behaviour II

This eigenvalue problem can be solved analytically by expanding the velocity in terms of vector spherical harmonics and the pressure in terms of scalar spherical harmonics (Meskauskas et al., 2011).

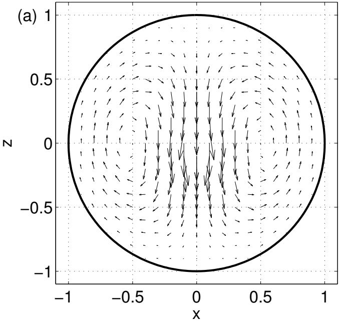

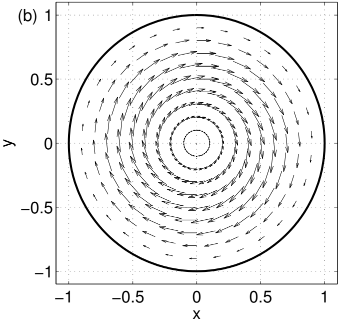

Spatial structure of the first two **eigenfunctions.**

Relaxation behaviour III

In order to determine the **eigenvalues** it is necessary to specify the model for the vitreous humour viscoelastic behaviour.

Two-parameter model

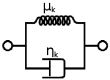

- dashpot: ideal viscous element
- spring: ideal elastic element

$$\tilde{G}(\lambda) = \mu_K + \lambda \eta_K.$$

Four-parameter model

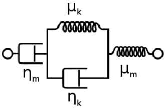

$$\tilde{G}(\lambda) = \frac{\lambda \eta_m \mu_m (\mu_K + \lambda \eta_K)}{(\mu_m + \lambda \eta_m)(\lambda \eta_m \mu_m / (\mu_m + \lambda \eta_m) + \mu_K + \lambda \eta_K)}$$

Some conclusions

- For all existing measurements of the rheological properties of the vitreous we find the **existence of natural frequencies of oscillation.**
- Such frequencies, for the least decaying modes, are within the range of physiological eye rotations ($\omega = 10 - 30$ rad/s).
- The two- and the four-parameter model lead to qualitatively different results:
  - **Two-parameter model:** only a finite number of modes have complex eigenvalues;
  - **Four-parameter model:** an infinite number of modes have complex eigenvalues.
- **Natural frequencies could be resonantly excited by eye rotations.**

The effect of the geometry I

Myopic Eyes

In comparison to emmetropic eyes, myopic eyes are

- larger in all directions;
- particularly so in the antero-posterior direction.

Myopic eyes bear **higher risks of posterior vitreous detachment and vitreous degeneration** $\rightarrow$ increased the risk of rhegmatogeneous retinal detachment.

The shape of the eye ball has been related to the degree of myopia (measured in dioptres D) by Atchison et al. (2005), who approximated the vitreous chamber with an ellipsoid.

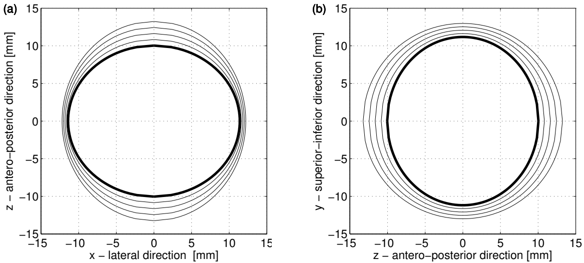

$$\text{width} = 11.4 - 0.04D,$$
$$\text{height} = 11.18 - 0.09D,$$
$$\text{length} = 10.04 - 0.16D.$$

(a) horizontal and (b) vertical cross sections of the domain for different degrees of myopia.

Formulation of the mathematical problem

Meskauskas et al., submitted to Invest. Ophthal. Vis. Scie.

Equation of the boundary

$$R(\vartheta, \varphi) = R_0(1 + \delta R_1(\vartheta, \varphi)),$$

where

- R_0 denotes the radius of the sphere with the same volume as the vitreous chamber;
- δ is a **small parameter** ($\delta \ll 1$);
- the maximum absolute value of R_1 is 1.

Expansion

We expand the velocity and pressure fields in therms of δ as follows

$$\mathbf{U} = \mathbf{U}_0 + \delta \mathbf{U}_1 + \mathcal{O}\left(\delta^2\right), \qquad P = P_0 + \delta P_1 + \mathcal{O}\left(\delta^2\right).$$

Solution

The solution at the order δ can be found analytically expanding R_1, $\mathbf{U}_1$ and P_1 in terms of spherical harmonics.

Myopic eyes I

Maximum stress on the retina as a function of the refractive error

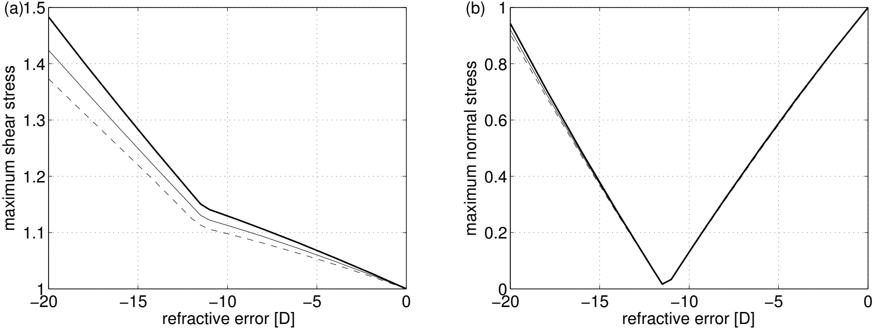

Maximum (over time and space) of the (a) tangential and (b) normal stress on the retina as a function of the refractive error in dioptres. **Values are normalised with the corresponding stress in the emmetropic (0 D) eye.** The different curves correspond to different values of the rheological properties of the vitreous humour taken from the literature.

Non-linear effects and implications for fluid mixing

Back to viscous fluids . . .

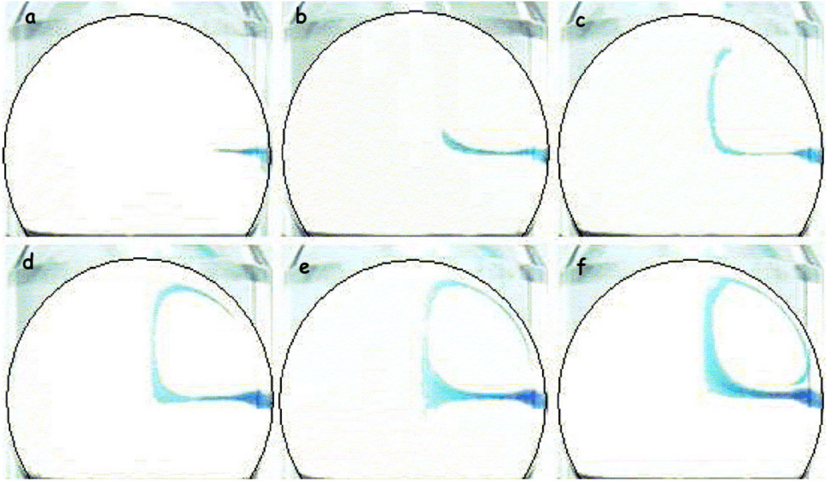

Flow visualisations on planes containing the axis of rotation.

Theoretical model I

Second order solution

$$\mathbf{u} = \varepsilon \mathbf{u}_1 + \varepsilon^2 \mathbf{u}_2 + \mathcal{O}(\varepsilon^3), \quad p = \varepsilon p_1 + \varepsilon^2 p_2 + \mathcal{O}(\varepsilon^3).$$

We decompose the velocity $\mathbf{u}_2$ and the pressure p_2 into their **time harmonics** by setting

$$\mathbf{u}_2 = \mathbf{u}_{20} + \left\{ \mathbf{u}_{22} e^{2it} + c.c. \right\}, \quad p_2 = p_{20} + \left\{ p_{22} e^{2it} + c.c. \right\}, \quad \mathbf{u}_1 \cdot \boldsymbol{\nabla} \mathbf{u}_1 = \mathcal{F}_0 + \left\{ \mathcal{F}_2 e^{2it} + c.c. \right\},$$

where $\mathbf{u}_{20}$, $\mathbf{u}_{22}$, p_{20}, p_{22}, $\mathcal{F}_0$ and $\mathcal{F}_2$ are independent of time.

Governing equations for the steady component

$$\nabla^2 \mathbf{u}_{20} - \boldsymbol{\nabla} p_{20} = \alpha^2 \mathcal{F}_0, \qquad \boldsymbol{\nabla} \cdot \mathbf{u}_{20} = 0, \tag{8a}$$

$$u_{20} = v_{20} = w_{20} = 0 \qquad (r = 1). \tag{8b}$$

Comparison between experimental and theoretical results I

- The steady streaming flow can be directly measured experimentally by cross-correlating images that are separated in time by a multiple of the frequency of oscillation.
- This procedure filters out from the measurements the oscillatory component of the flow.

Repetto et al. (2008), J. Fluid Mech.

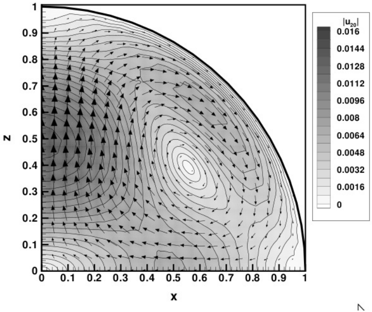

Numerical

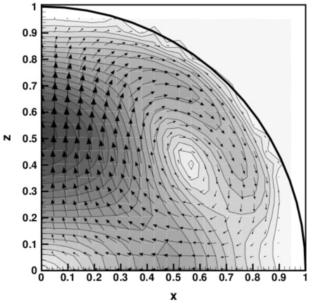

Experimental

Conclusions

- Eye movements during reading: $\approx$ 0.16 rad, $\approx 63\ s^{-1}$ (Dyson et al., 2004).
- Kinematic viscosity of the vitreous: $\nu \approx 7 \times 10^{-4}$ m^{2}s^{-1} (Lee et al., 1992).
- Eye radius: $R_0 = 0.012$ m.
- Womersley number: $\alpha = 3.6$.
- Streaming velocity: $U = \varepsilon^2 \delta \max(|\mathbf{u}_{21}^{(0)}|) \approx 6 \times 10^{-5}$ m s^{-1}.
- Diffusion coefficient of fluorescein: $D \approx 6 \times 10^{-10}$ m s^{-1} (Kaiser and Maurice, 1964)

Peclèt number: $Pe \approx 1200$.

In this case advection is much more important than diffusion!

Stability of the interface between aqueous humor and vitreous substitutes after vitreoretinal surgery

Retinal detachment

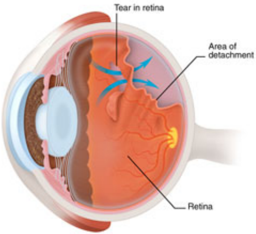

Warning signs of retinal detachment:

- Flashing lights.
- Sudden appearance of floaters.
- Shadows on the periphery of your vision.
- Gray curtain across your field of vision.

Vitrectomy

The vitreous may be completely replaced with tamponade fluids: silicon oils, water, gas, ...

- Denoted **tamponade liquids**
- Purpose: Induce an instantaneous interruption of an open communication between the subretinal space/retinal pigment epithelial cells and the pre-retinal space.
- Healing: a scar should form as the cells absorb the remaining liquid.

Fluids commonly used as a vitreous substitutes

- **Silicone oils**;
  - $960 \leq \rho^* \leq 1290$ kg/m^3
  - $10^{-4} \leq \nu^* \leq 5 \times 10^{-3}$ m/s^2
  - $\sigma^* \approx 0.05$ N/m
- **Perfluorocarbon liquids**;
  - $1760 \leq \rho^* \leq 2030$ kg/m^3
  - $8 \times 10^{-7} \leq \nu^* \leq 8 \times 10^{-6}$ m/s^2
  - $\sigma^* \approx 0.05$ N/m
- **Semifluorinated alkane liquids**;
  - $1350 \leq \rho^* \leq 1620$ kg/m^3
  - $4.6 \times 10 \leq \nu^* \leq 10^{-3}$ m/s^2
  - $0.035 \leq \sigma^* \leq 0.05$ N/m

The choice of tamponade liquid depends on the specific case

- The tabulated fluids are **immiscible** with water and commonly used in surgery
- A lighter fluid (cf. water) is used to tamponade in the upper part
- A heavier fluid is used to tamponade in the lower part
- High surface tension is preferred to a low value (**EXPERIENCE**)
- High value of viscosity (cf. water) is preferred to a low value (**EXPERIENCE**)

What could happen otherwise ?

Emulsification

Emulsification leads to loss of vision, **not satisfactory**

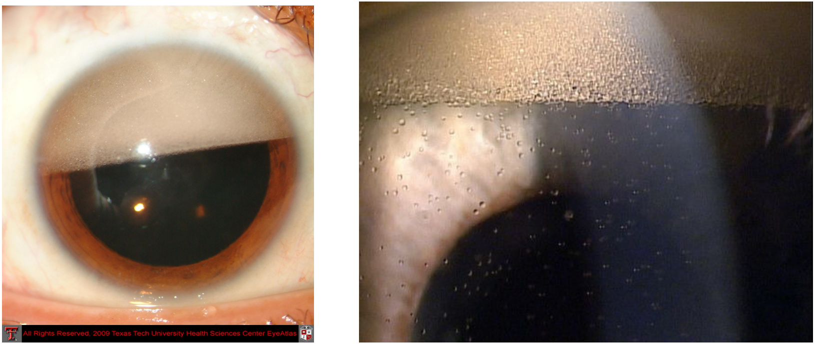

Figure: Emulsification of vitreous substitutes in the vitreous chamber

Summary & Motivation

Summary

- From **experience** it is known that tamponade fluids with **high surface tension** and **high viscosity** (compared to water) are less prone to emulsify
- It is also know that initially "good" tamponade fluids tend to change with time, for instance a decrease of surface tension due to **surfactants**, which leads to emulsification.
- It is generally believed that **shear stresses** at the tamponade fluid-aqueous **interface** generated during eye rotations play a crucial role in the generation of an emulsion.
- The tamponade liquid needs to stay for a period of months so it is of interest to know how emulsification can be avoided.

Our analysis

- We want understand how emulsification, or the initial stages leading to emulsification, are related to the parameters (surface tension, viscosity, density, real conditions).
- As a first study we focus on the **stability characteristics of the interface** in order to see if it has any role.
- A linear stability analysis, of wave like solutions, is used.

Mathematical model I

The geometry

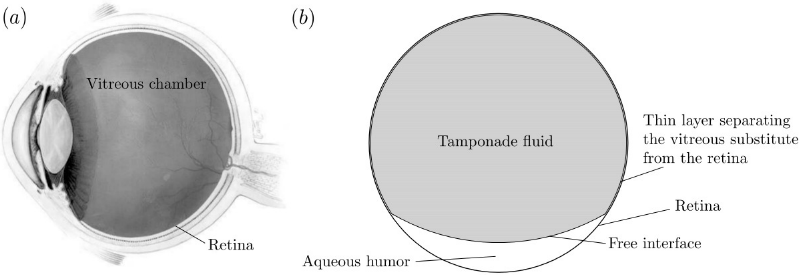

Mathematical model II

Underlying assumptions

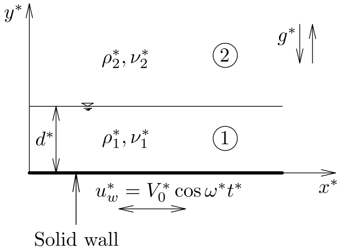

Figure: Geometry of the problem

- $d^* << R^*$
- 2D-model;
- flat wall oscillating harmonically;
- semi-infinite domain;
- small perturbations;
- quasi-steady approach.

Scaling and Dimensionless Parameters

$$\mathbf{x} = \frac{\mathbf{x}^*}{d^*}, \quad \mathbf{u_i} = \frac{\mathbf{u_i}^*}{V_0^*}, \quad p_i = \frac{p_i^*}{\rho_1^* V_0^{*2}}, \quad t = \frac{V_0^*}{d^*} t, \quad \omega = \frac{d^*}{V_0^*} \omega^*$$

$$m = \frac{\mu_2^*}{\mu_1^*} \qquad \gamma = \frac{\rho_2^*}{\rho_1^*}$$

$$R = \frac{V_0^* d^*}{\nu_1^*} \qquad Fr = \frac{V_0^*}{\sqrt{g^* d^*}}$$

$$S = \frac{\sigma^*}{\rho_1^* d^* V_0^{*2}}$$

Basic flow

Analytical solution

$$U_1(y,t) = (c_1 e^{-ay} + c_2 e^{ey}) e^{i\omega t} + c.c.,$$
$$U_2(y,t) = c_3 e^{-by} e^{i\omega t} + c.c.,$$
$$\frac{\partial P_1}{\partial y} = -Fr^{-2},$$
$$\frac{\partial P_2}{\partial y} = -\gamma Fr^{-2},$$

where

$$a = \sqrt{i\omega R}, \qquad b = \sqrt{\frac{i\gamma\omega R}{m}}.$$

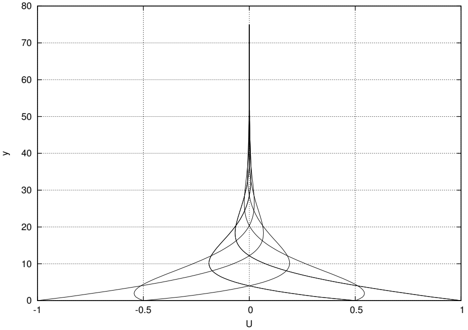

Linear stability analysis

Flow decomposition:

$$u_i = U_i + u_i{}', \; v_i = v_i{}' \quad p_i = P_i + p_i'$$

Boundary conditions:

$$u_1'(0,t) = v_1'(0,t) = 0 \quad \text{and} \quad u_2'(y,t) \to 0, \; v_2'(y,t) \to 0 \quad \text{as} \quad y \to \infty$$

Interface: $(y^* = d^*)$ introducing also the perturbation of the interface η'

- Continuity of the perturbation velocity components across the interface
- Continuity of the tangential stress of across the interface
- The wall normal stress is balanced by the surface tension

Wave-like solutions are assumed:

$$\xi_i = e^{i\alpha(x-\Omega t)}\hat{\xi}_i(y,\tau) + c.c$$

where

$$0 \leq \tau \leq 2\pi/\omega$$

The system of equations is reduced introducing the perturbation stream function giving **two Orr-Sommerfeld equations**, discretized using finite differences, solved using an inverse iteration algorithm.

Range of variability of the dimensionless parameters

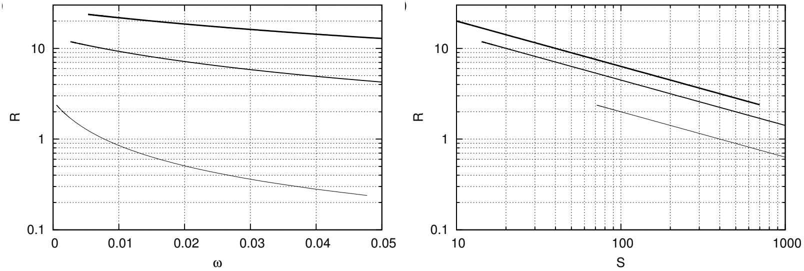

Figure: Relationship between R and ω and S and ω obtained adopting feasible values of eye movement. From thin to thick curves: $d = 1 \times 10^{-5}$m, $d = 5 \times 10^{-5}$m, $d = 1 \times 10^{-4}$m

Neutral Curves

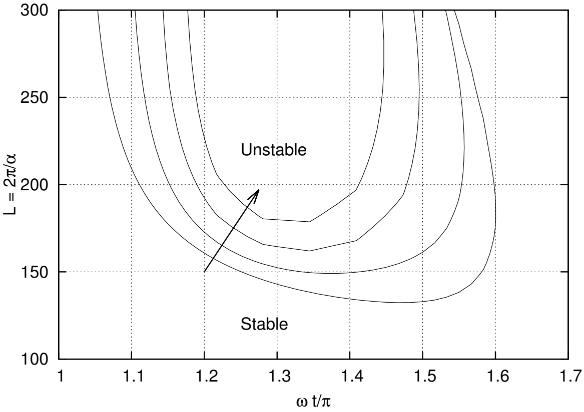

Figure: $S = 14$, $\gamma = 1.0$, $R = 12$, $\omega = 0.003$

The arrow indicates increasing value of the parameter m (viscosity ratio).

Dependence on m

The **shortest** unstable wave length as a function of the viscosity ratio m.

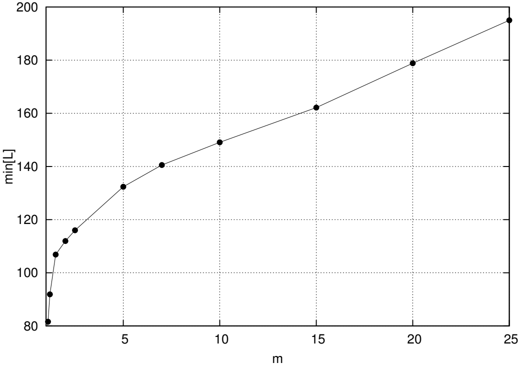

Figure: $S = 14$, $\gamma = 1.0$, $R = 12$, $\omega = 0.003$

Dependence on S

The **shortest** unstable wave length as a function of the surface tension S.

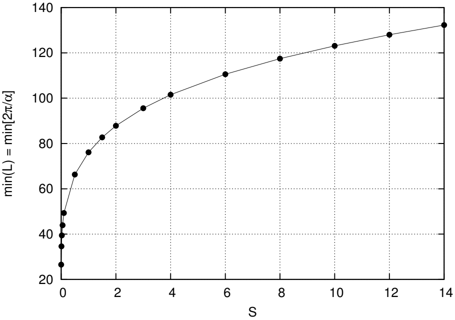

Figure: $R = 12$, $m = 5.0$, $\gamma = 1.0$, $\omega = 0.003$

Dependence of R

The **shortest** unstable wave length as a function of the Reynolds number R.

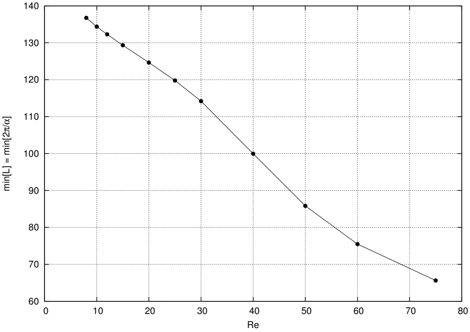

Figure: $S = 14$, $m = 5.0$, $\gamma = 1.0$, $\omega = 0.003$

Dependence on γ

The **shortest** unstable wave length as a function of the density ratio γ.

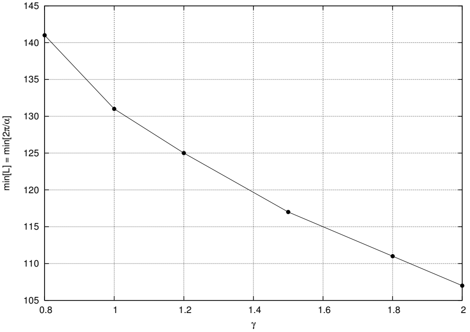

Figure: $S = 14$, $m = 5.0$, $R = 12$, $\omega = 0.003$

Conclusions and Continuation

Monitoring the shortest unstable wave length (critical wave length) we have seen that:

- Increasing the viscosity, ratio the critical wave length increases (**stabilizing for the Eye**)
- Increasing the surface tension, the critical wave length increases (**stabilizing for the Eye**)
- Increasing the Reynolds no., the critical wave length decreases (**destabilizing for the Eye**)
- Increasing the density ratio, the critical wave length decreases (**destabilizing for the Eye**)
- The first two is "in line" with realistic observations.
- For realistic values of $R, S, \gamma, m, \omega, d^*$ the critical wave length ≈ 6 mm, which is about half the Eye radius.
- However, the growth rate is instantaneous and the waves unstable only during certain intervals of one period. (cf. turbulent burst in the classical Stokes II problem). No sustained growth over one period is guaranteed.
- This analysis is far from explaining the onset of emulsion but a first step to rule out (or not) different physical mechanisms.

Next step...

- Budget of disturbance kinetic energy (Reynolds-Orr) (ongoing)
- Floquet analysis (ongoing)

References I

D. A. Atchison, N. Pritchard, K. L. Schmid, D. H. Scott, C. E. Jones, and J. M. Pope. Shape of the retinal surface in emmetropia and myopia. *Investigative Ophthalmology & Visual Science*, 46(8):2698–2707, 2005. doi: 10.1167/iovs.04-1506.

T. David, S. Smye, T. Dabbs, and T. James. A model for the fluid motion of vitreous humour of the human eye during saccadic movement. *Phys. Med. Biol.*, 43:1385–1399, 1998.

R. Dyson, A. J. Fitt, O. E. Jensen, N. Mottram, D. Miroshnychenko, S. Naire, R. Ocone, J. H. Siggers, and A. Smithbecker. Post re-attachment retinal re-detachment. In *Proceedings of the Fourth Medical Study Group, University of Strathclyde, Glasgow*, 2004.

B. Lee, M. Litt, and G. Buchsbaum. Rheology of the vitreous body. Part I: viscoelasticity of human vitreous. *Biorheology*, 29:521–533, 1992.

J. Meskauskas, R. Repetto, and J. H. Siggers. Oscillatory motion of a viscoelastic fluid within a spherical cavity. *Journal of Fluid Mechanics*, 685:1–22, 2011. doi: 10.1017/jfm.2011.263.

C. S. Nickerson, J. Park, J. A. Kornfield, and H. Karageozian. Rheological properties of the vitreous and the role of hyaluronic acid. *Journal of Biomechanics*, 41(9):1840–6, 2008. doi: 10.1016/j.jbiomech.2008.04.015.

R. Repetto, A. Stocchino, and C. Cafferata. Experimental investigation of vitreous humour motion within a human eye model. *Phys. Med. Biol.*, 50:4729–4743, 2005. doi: 10.1088/0031-9155/50/19/021.

References II

R. Repetto, J. H. Siggers, and A. Stocchino. Steady streaming within a periodically rotating sphere. *Journal of Fluid Mechanics*, 608:71–80, August 2008. doi: 10.1017/S002211200800222X.

R. Repetto, J. H. Siggers, and A. Stocchino. Mathematical model of flow in the vitreous humor induced by saccadic eye rotations: effect of geometry. *Biomechanics and Modeling in Mechanobiology*, 9(1):65–76, 2010. ISSN 1617-7959. doi: 10.1007/s10237-009-0159-0.

K. Swindle, P. Hamilton, and N. Ravi. In situ formation of hydrogels as vitreous substitutes: Viscoelastic comparison to porcine vitreous. *Journal of Biomedical Materials Research - Part A*, 87A(3):656–665, Dec. 2008. ISSN 1549-3296.